

Link between static radial tire stiffness and the size of its contact surface and contact pressure

M. Kučera^{1,*} M. Helexa¹ and J. Čedík²

¹Technical University in Zvolen, Faculty of Environmental and Manufacturing Technology, T.G. Masaryka 24, SK 96053 Zvolen, Slovak Republic.

²Czech University of Life Sciences Prague, Faculty of Engineering, Kamýcká 129, CZ 16521, Praha – Suchbátka, Czech Republic

*Correspondence: marian.kucera@tuzvo.sk

Abstract. The article is devoted to the description of the experimental results regarding the measurement of static radial deformation characteristics of the selected tire and its impact on the size of the contact surface and contact pressure. The given measurement was carried out on the diagonal tire Mitas TS05 10.0/75-15.3 PR10 in the area of the soil test channel. The radial deformation characteristics of the tires in question were determined for inflation pressures of 300 kPa, 220 kPa, 160 kPa and 100 kPa, with a radial stress of the tire varying in the range of 567.9 kg to 1025.09 kg. The prints of the tire's contact surfaces were made at the same time for the corresponding inflation pressure and the corresponding radial stress. The size of these prints was subsequently planimeterized by the digital polar planimeter Koizumi KP-90N. The values of the medium contact pressure on a solid support were subsequently calculated from the tire radial stress values and the obtained contact surfaces. The calculated static radial stiffness values were obtained through the linearization of the measured deformation characteristics according to Jante. The course of the deformation characteristics and the calculation of static radial stiffness imply that static radial stiffness is significantly dependent on the tire inflation pressure. A suppler tire structure at a lower inflation pressure allows for greater values of the contact surfaces and lower values of contact pressures. This feature can be used when selecting appropriate tire inflation pressures when driving off-road to reduce soil degradation and improving the vehicle's passability through the terrain.

Key words: terramechanics, landscape, mobile machines, wheeled chassis.

INTRODUCTION

The radial stiffness of tires (whether static or dynamic) does not only affect the cushioning of the energy means in the terrain, but also other characteristics of the tire relating to its contact with the surface of the terrain it moves on. It affects the size of the tire's contact area, the size of the contact pressure, the size of the internal as well as external rolling resistance component, and thus affects the energy losses in the overall performance applied to the wheels of mobile working means (Antille et al., 2013; Abrahám et al., 2014). Radial tire deformation characteristics of mobile technology used in forestry and agriculture are therefore an important attribute for solving contact problems between the tire and the surface. The size of the contact pressure is influenced mainly by the size of the tire's contact area and its normal stress. The size and course of

the tire's contact pressure greatly affects how this will behave, for example, on soil, how it will damage the soil (e.g. by compression or excessive slipping) and what driving and operating properties the mobile means will achieve with it under the given soil conditions (Braunack, 2004; Čedík & Pražan, 2015). Research tire deformation characteristics was dealt with in the past by several authors, for example, Dočkal et al. (1998), Zhang et al. (2002), Krmela (2008), Koutný (2009), and, who in their work also highlighted the impact of tire deformation properties on their driving and contact properties. In the research of mutual ties between the tire wheel deformation characteristics and contact variables, especially the size of the contact area and the contact pressure distribution on a solid support, progressive methods of research using various physical principles of tactile sensing elements have also been used. These allow precisely determining the composition of the contact pressure in the tire's contact area with the surface, and accurately determine the size of the contact area. Thus the conceived work is indicated by authors, such as De Beer & Fisher (1997), who applied a tactile matrix consisting of strain-gauge sensing elements to map the contact area and contact pressure. An interesting application of tactile sensing elements, or a force sensor consisting of tactile sensing elements, was introduced by the authors Roth & Darr (2012). To monitor the contact pressure of the tire and the size of the contact surface, they used Tekscan FlexiForce tactile force transducers, which they installed directly on the tractor tire tread close to the herringbone tread figures. What is interesting about this work is the fact that they used the above method of installing the sensors to monitor the contact voltage between the tire and the soil surface. Optical methods are also used for the investigation of contact tasks and their relation with the deformation characteristics of tires. The utilization of holographic interferometry methods in this area is described by authors such as Castillo et al. (2006).

As seen from the above brief overview, the topic is still relevant and it is currently being dealt with through advanced technologies brought by microelectronics. In this article, we will also try to suggest a link between the radial deformation characteristics of the selected tire and the size of the contact area and contact pressure.

MATERIALS AND METHODS

We investigated the radial deformation characteristics of the selected tire for different values of inflation pressure and different values of vertical stress in soil test channels (Fig. 1). The vertical load on the tire was inferred through steel weights from the value of 567.90 kg to 1,025.09 kg. We selected the stress on the tire so that at a given tire inflation pressure we would not exceed the maximum stress indicated by the manufacturer. The construction of the supporting frame of the wheel (Item 3, Fig. 1) does not allow to achieve a tire stress lower than 480 kg. It is due to the fact that the entire drive mechanism of the tested wheel is mounted on this item, which is used in the traction tire tests (together with Items 5 and 6, Fig. 1). As a test tire we selected a Mitas TS05 10.0/75-15.3 PR10 ply tire with a tread profile. Its basic technical parameters are listed in the following Table No.1.

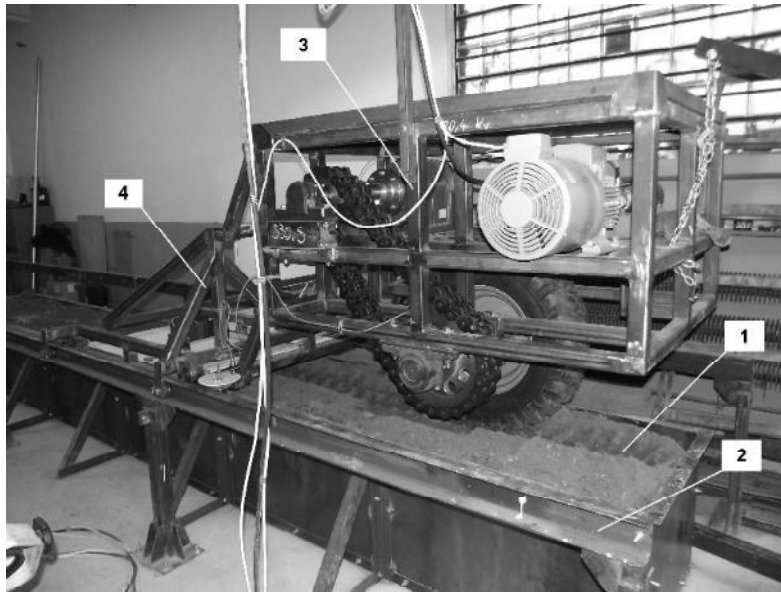


Figure 1. Soil test channel: 1 – soil test channel’s body (frame); 2 – side guiding; 3 – wheel support frame; 4 – the guide frame, 5 – tensile force sensor; 6 – brake device.

Table 1. Basic technical parameters of the monitored tire

Tire type	Dimension	PR	Tread profile	Rim	Width (mm)	Diameter (mm)	Radius (mm)	Rolling circumference (mm)
itaMs	TS05 10.0/75-15.3 PR10	10	TS 05	9.00 x 15.3	264	790	395	2,295

We have carried out the actual measurement of the radial deformation characteristics so that we lifted the supporting frame with the mounted tire using a workshop crane with a lifting capacity of 5,000 kg, and supported the wheel on the evened-out soil surface with a 15 mm thick steel substrate. We examined the actual tire compression using an altimeter with a nominal size of 1,000 mm. In addition to these measurements, we investigated the necessary parameters of the tire’s contact area with the substrate. We imprinted the contact surface of the tire on rough drawing paper, painting it with ink beforehand. We always made two imprints for the given load and tire inflation pressure. One of the contact surfaces of the tire with the solid substrate and the second of the imprint surface, which is closer to the contact area, is on the soil surface. We then determined the size of the contact surface and the tire contact surface via a Koizumi KP-90N digital polar planimeter (Fig. 2). The obtained radial tire deformation characteristics were obtained for the following inflation pressures: 300 kPa, 220 kPa, 160 kPa and 100 kPa.

From the obtained deformation characteristics, we then calculated the static radial stiffness of the examined tire. The course of dependence of the vertical stress on the tire deformation is a second degree polynomial in the form:

$$Q = A.y + B.y^2 \text{ [N]} \quad (1)$$

where: Q – vertical stress on the tire, [N]; A, B – functional dependence constants $Q(y)$, [-]; y – vertical deformation of the tire, [m].

The linearization of the dependence was carried out according to Jante (Cvekl et al., 1976) on the basis of the statement that the work expended to deform the tire, expressed as follows:

$$E_p = \int_0^{y_{\max}} (A.y + B.y^2) dy \text{ [J]} \quad (2)$$

is as big as the work expended to deform the tire in a linearized form. The sought constant of the linearized stress process stiffness then follows from the following equation:

$$E_p = \int_0^{y_{\max}} c.y dy = \frac{1}{2}.c.y_{\max}^2 \text{ [J]} \quad (3)$$

where: E_p – work expended to deform the tire, [J]; c – radial static stiffness of the tire, [N m^{-1}]; y_{\max} – maximum vertical tire deformation at the corresponding stress and given inflation pressure, [m].



Figure 2. Koizumi KP-90N digital polar planimeter.

We then calculated the mean contact pressure values from the values of the measured contact surface and vertical load.

RESULTS

The results of the measurements and calculation of work expended for the tire deflection and static radial stiffness of the tire are shown in Table 2. All the calculations and reported functional dependencies of work were developed in a MS Excel spreadsheet. The measured tire deformation characteristics for individual inflation pressures are graphically illustrated in Fig. 3. The given functional dependencies of the tire stress depending on the vertical deformation can be approximated by a second degree polynomial. The obtained functional dependencies, indicating the coefficient of determination, are shown in Table 3.

Table 2. Measured and calculated results, the Mitas TS05 10.0/75-15.3 PR10 tire

Load (kg)	Normal Force (N)	Pressure (kPa)	Tire rolling radius (mm)	Deformation of tire (mm)	Work expended on deformation (J)	Stiffness (N m ⁻¹)
1,025.09	10,056.13	300.00	376.00	19.00	94.77	525,000
847.14	8,310.44	300.00	379.00	16.00	69.19	
709.30	6,958.23	300.00	381.00	14.00	54.82	
567.90	5,571.10	300.00	384.00	11.00	36.88	
0.00	0.00	300.00	395.00	0.00	0.00	
1,025.09	10,056.13	220.00	373.00	22.00	126.46	522,500
847.14	8,310.44	220.00	377.00	18.00	90.53	
709.30	6,958.23	220.00	380.00	15.00	67.98	
567.90	5,571.10	220.00	384.00	11.00	43.18	
0.00	0.00	220.00	395.00	0.00	0.000	
847.14	8,310.44	160.00	376.00	19.00	76.39	423,200
709.30	6,958.23	160.00	379.00	16.00	53.57	
656.48	6,440.07	160.00	380.00	15.00	46.88	
567.90	5,571.10	160.00	382.00	13.00	34.86	
0.00	0.00	160.00	395.00	0.00	0.000	
847.14	8,310.44	100.00	369.00	26.00	64.99	192,300
709.30	6,958.23	100.00	372.00	23.00	42.20	
656.48	6,440.07	100.00	373.00	22.00	35.52	
567.90	5,571.10	100.00	375.00	20.00	23.53	
0.00	0.00	100.00	395.00	0.00	0.00	

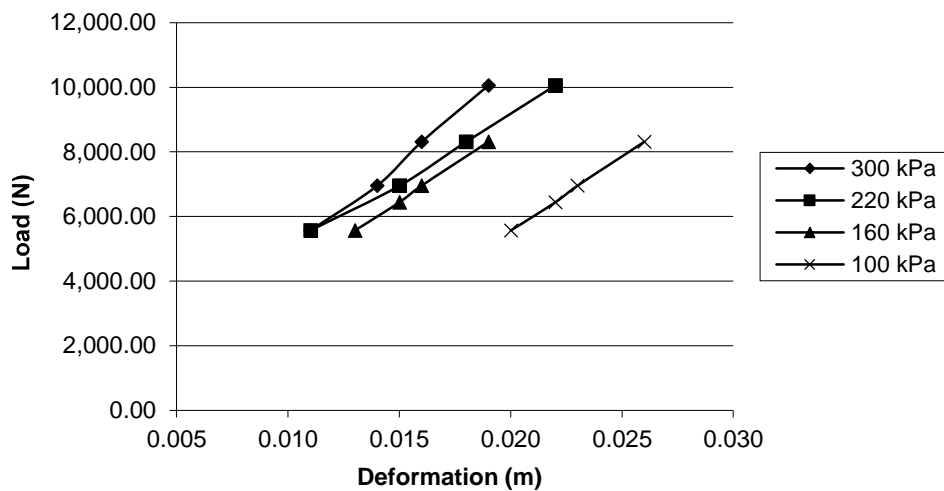


Figure 3. Radial deformation characteristics of the examined tire Mitas TS05 10.0/75-15.3 PR10

We subsequently used the coefficient values of these obtained approximation functional dependencies (Table 3) to calculate the potential energy (deformation work) according to Equation 2 and to calculate the radial static stiffness of the tire according to Equation 3.

Table 3. Dependencies of the deformation characteristics for the Mitas TS05 10.0/75-15.3 PR10

Tire inflation pressure	Function	R ²
300 kPa	$y = 1E+07.x^2 + 208,866.x + 1,800,2$	0.9977
220 kPa	$y = 6E+06.x^2 + 199,416.x + 2,586.4$	0.9993
160 kPa	$y = 1E+06.x^2 + 424,967.x - 136.92$	0.9995
100 kPa	$y = 1E+06.x^2 + 410,363.x - 3,060.6$	0.9995

Note: y – vertical load on the tire, [N] x – tire deformation, m.

The results of measuring the contact surface size and the contact area of the examined tire for individual stresses and tire inflation pressures are shown in Table 4. This table also shows the calculation of the mean contact pressure for individual stresses and the imprint surfaces, as well as the tire contact surface. Unfortunately at present we do not have a device that would allow us to measure the value of mean contact pressure or to measure the total contact pressure distribution in the tire's contact area, so we just proceeded to their calculation.

DISCUSSION

The dependence of tire deflection on the stress (Fig. 3) is non-linear and describable by the polynomial of the second degree (quadratic function). The indicated static radial stiffness values were obtained by the linearization of these functions according to Jante (Cvekl et al., 1976), Table 2. The dependence of the tire imprint area on the stress and inflation pressure (Fig. 4) shows that the imprint area clearly increases with an increasing

radial load and decreasing tire inflation pressure. The maximum is reached at an inflation pressure of 100 kPa and a maximum stress of 847.14 kg. In this dependence, we may discern some variation consisting in a significant reduction of the tire contact area depending on the stress and inflation pressure when inflated to 160 kPa. This may be caused by certain flaws in the performance of the measurement or a small number of performed measurements.

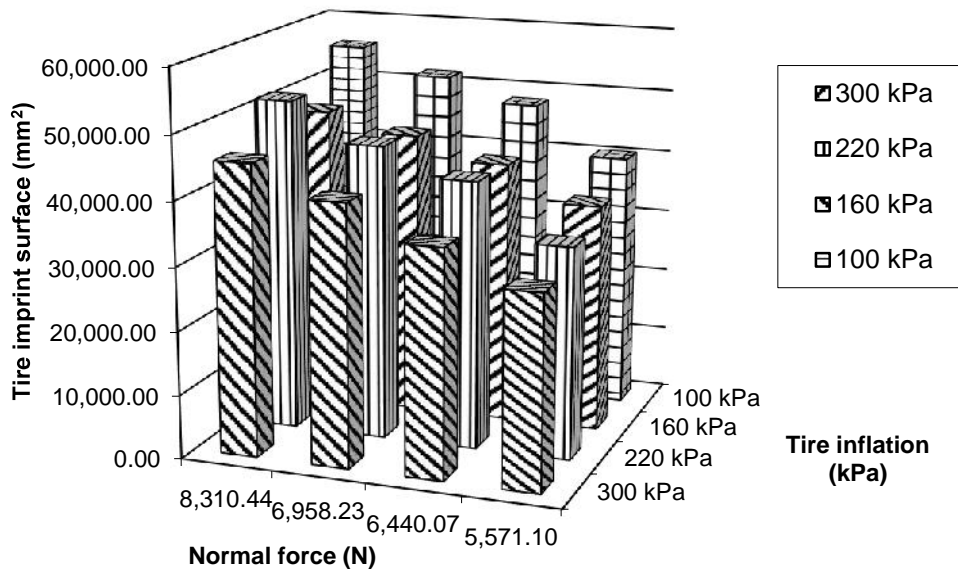


Figure 4. Dependency of the tire imprint surface on the normal force and inflation pressure.

The tire contact area with a solid substrate depending on the stress and inflation pressure behaves essentially the same as in the previous case.

In the dependence of the mean tire contact pressure on the load and inflation pressure (Fig. 5) we can observe that the mean contact pressure of the tire increases not only due to increasing vertical stress, but also due to the rising inflation pressure of the tire. It reaches its maximum at 300 kPa inflation pressure and a vertical stress of 1,025.09 kg. The dependency of the mean tire contact pressure on a hard substrate depending on the stress and inflation pressure for a contact surface has a similar course as in the previous example.

Regarding the mutual size proportion of the imprint surface and the tire contact area (Table 4), based on the measured data we can say that the tire contact area was on average 3.14 times smaller than the imprint surface. The contact surface essentially represents a contact area of the tread profile on a solid substrate. It is affected by the fullness of the tread profile, i.e. the number and arrangement of gear figures of the tires with an arrow tread profile.

Table 4. The results of the size measurements of the contact surface and the monitored tire's contact area

Load (kg)	Normal force (N)	Inflation pressure (kPa)	Track width (mm)	Track length (mm)	Deformation (mm)	Imprint surface (mm ²)	Contact area (mm ²)	Mean contact pressure (imprint) (Pa)	Mean contact pressure (contact) (Pa)
1,025.09	10,056.13	300.00	230.00	245.00	19.00	45,561.19	17,085.25	220,717.08	588,585.65
847.14	8,310.44	300.00	220.00	220.00	16.00	40,820.27	14,115.40	203,586.19	588,750.12
709.30	6,958.23	300.00	212.00	205.00	14.00	35,475.40	12,775.18	196,142.48	544,668.10
567.90	5,571.10	300.00	200.00	190.00	11.00	30,260.13	9,165.63	184,106.91	607,824.99
0.00	0.00	300.00	0.00	0.00	0.00	0.00	0.00	0.00	0.00
1,025.09	10,056.13	220.00	228.00	260.00	22.00	52,120.40	15,450.52	192,940.44	650,860.48
847.14	8,310.44	220.00	222.00	229.00	18.00	46,196.07	13,605.38	179,895.03	610,820.38
709.30	6,958.23	220.00	221.00	223.00	15.00	41,888.78	12,634.47	166,112.09	550,734.06
567.90	5,571.10	220.00	210.00	188.00	11.00	33,182.52	10,200.62	167,892.58	546,152.98
0.00	0.00	220.00	0.00	0.00	0.00	0.00	0.00	0.00	0.00
847.14	8,310.44	160.00	221.00	243.00	19.00	47,674.24	15,995.35	174,317.27	519,553.71
709.30	6,958.23	160.00	220.00	225.00	16.00	44,865.21	14,285.08	155,091.95	487,097.94
656.48	6,440.07	160.00	219.00	222.00	15.00	41,385.37	13,875.04	155,612.24	464,147.85
567.90	5,571.10	160.00	218.00	200.00	13.00	35,905.52	11,465.00	155,159.96	485,922.29
0.00	0.00	160.00	0.00	0.00	0.00	0.00	0.00	0.00	0.00
847.14	8,310.44	100.00	220.00	285.00	26.00	55,756.47	18,910.41	149,048.95	439,463.95
709.30	6,958.23	100.00	218.00	256.00	23.00	51,681.50	15,579.77	134,636.82	446,619.75
656.48	6,440.07	100.00	219.00	234.00	22.00	48,005.95	15,140.11	134,151.50	425,364.81
567.90	5,571.10	100.00	220.00	210.00	20.00	40,330.40	12,700.44	138,136.47	438,654.02
0.00	0.00	100.00	0.00	0.00	0.00	0.00	0.00	0.00	0.00

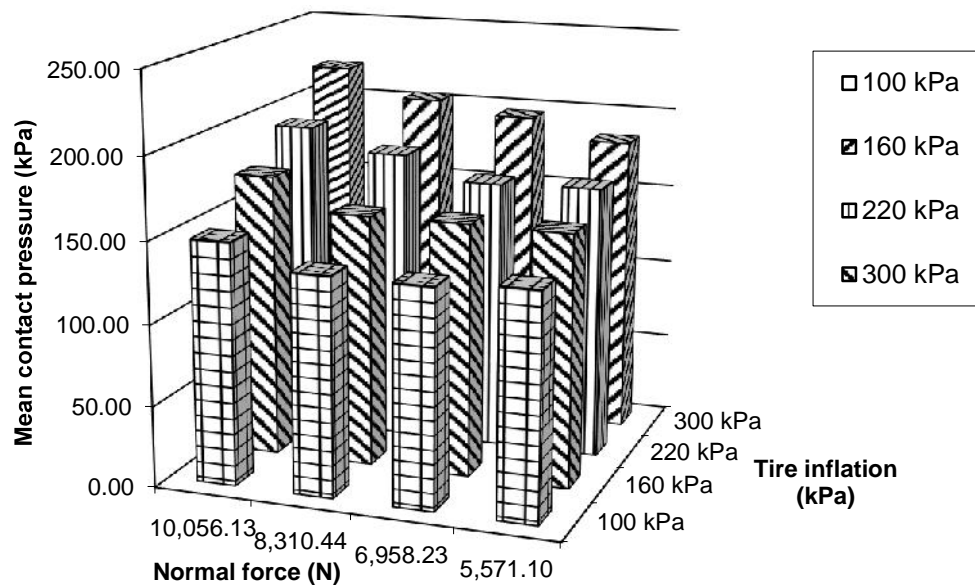


Figure 5. Dependency of the mean tire contact pressure (Imprint surface) on the stress and inflation pressure.

As mentioned above, we just calculated the value of the mean contact pressure using the known value of the vertical tire stress and the measured imprint surface and the contact area. Currently we do not have technical equipment that would allow us to measure this parameter or determine the distribution of the contact pressure in the tire's contact area. Several authors suggest in their work that the mean contact pressure value is approximately equal to the tire inflation pressure (Faria & Oden, 1992; Grečenko, 1995; Noor & Peters, 1995;). However, this ideal situation would be valid if the tire was perfectly elastic. In reality, it is not. Our results showed the following. At a tire inflation pressure of 100 kPa, the mean contact pressure value when considering the imprint area was around 127 kPa to 189 kPa, which is consistent with the theory that the real value of the mean contact pressure in a real tire is always greater than the tire inflation pressure. At a tire inflation pressure of 160 kPa, the values of mean contact pressures were approximately on a level equal to the tire inflation pressures. At the inflation pressure of 220 kPa, the contact pressure was somewhat lower, moving at 168 kPa to 193 kPa. At a tire inflation pressure of 300 kPa we obtained mean contact pressure values of 184 kPa to 221 kPa.

Given that the tire contact area is on average 3.14 times smaller than the entire imprint area, the mean contact pressure values are also greater by this fold, ranging from 440 kPa at the tire inflation pressure of 100 kPa, to 588 kPa at the inflation pressure of 300 kPa and maximum stress.

The course of the deformation characteristics and the calculation of static radial stiffness (Fig. 2, Table 2) show that this is heavily dependent on the tire inflation pressure. The lower the tire inflation pressure, the more pliable the tire (lower radial stiffness). At inflation pressures of 100 kPa it is nearly 2 times lower than at 300 kPa. The radial static stiffness value and thus the flexibility is affected not only by the tire

inflation pressure, but also the very structure of the tire. It depends on whether the structure of the tire is radial or diagonal, the number of cord layers, and the material of cord layers.

A suppler tire structure at lower inflation pressure allows for greater values of the contact surfaces (at a given load) and lower values of contact pressures (Schreiber & Kutzbach, 2008; Barosa & Magalhães, 2015). This feature can be used when selecting an appropriate tire inflation pressure for off-road driving on a flexible substrate to reduce soil degradation and reduce the rolling resistance of the tire. On a solid surface, however, the reduced tire inflation pressure at the given stress clearly leads to the increased internal component of the tire rolling resistance. Here, therefore, we strive to achieve that the tire is adequately stiff (inflated to the highest pressure proportionate to its maximum stress), which provides an acceptable rolling resistance value while reaching the optimum life.

CONCLUSION

In conclusion, we would like to mention that the very soil test channel which we conducted our measurement on is not quite suitable for detecting the deformation characteristics of tires. The main limiting parameter is the fact that it does not allow us to ensure the lower stress of the observed tire than 480 kg without having to dismount the wheel drive mechanism. As mentioned above, the vertical stress on the tire is inferred here by means of mechanical weights, their manual handling cumbersome, time-consuming and physically strenuous for the equipment operation staff. A device called the static adhezor is more preferable for verifying the deformation characteristics of the tire wheels, enabling the accurate measurement of individual deformation characteristics (not only in the radial direction) of the tires. Our workplaces, however, currently do not have this piece of equipment. In the future we would like to continue in the given research area of deformation characteristics and refine the given measurements to the desired level.

The measurements performed by us do not provide any fundamentally new results, but confirm the view that the tire inflation pressure, as well as the selection of an appropriate tire size for specific mobile work equipment, plays an important role in the energy efficiency of these machines. We think that we have managed to suggest a link between the radial stiffness of the tire and the size of its contact area and contact pressure. These characteristics of tires must be reviewed even before the tire is fitted to the specific mechanization means. Based on the results of this verification, it is then possible to determine the tire's suitability for the particular mechanization means, so that its work in the terrain is as efficient as possible.

ACKNOWLEDGEMENT. The paper was created within the solution of grant project VEGA MŠ SR No. 1/0676/14.

REFERENCES

- Abrahám, R., Majdán, R., Šima, T., Chrastina, J. & Tulík, J. 2014. Increase in tractor drawbar pull using special wheels. *Agronomy Research* **12**(1), 7–16.
- Antille, D.L., Ansorge, D., Dresser, M.L. & Godwin, R.J. 2013. Soil displacement and soil bulk density changes as affected by tire size. *Transactions of the ASABE* **56**(5), 1683–1693.
- Barbosa, L.A.P. & Magalhães, P.S.G. 2015. Tire tread pattern design trigger on the stress distribution over rigid surfaces and soil compaction. *Journal of Terramechanics* **58**(1), 27–38.
- Braunack, M.V. 2004. A tyre option for sugarcane haulout trucks to minimise soil compaction. *Journal of Terramechanics* **41**(4), 243–253.
- Castillo, J., Pérez de la Blanca, A., Cabrera, J.A. & Simón, A. 2006. An optical tire contact pressure test bench. *Vehicle System Dynamics* **44**(3), 207–211.
- Čedík, J. & Pražan, R. 2015. Comparison of tyre for self-propelled sprayers. *Agronomy Research* **13**(1), 53–62.
- Cvekl, Z. & Dražan, F. 1976. *Teoretické základy transportních zařízení (Theoretical foundation of transport equipment)*. SNTL/Alfa, Praha-Bratislava, 320 pp. (in Czech)
- De Beer, M. & Fisher, C. 1997. Contact stresses of pneumatic tires measured with the vehicle-road surface pressure transducer array (VRSPTA) system for the University of California at Berkeley (UCB) and the Nevada Automotive Test Center (NATC). *Confidential contract research report CR-971053*, Division of Roads and Transport Technology, CSIR, Pretoria, South Africa, 13pp.
- Dočkal, V., Kovanda, J. & Hrubec, F. 1998. *Pneumatiky (Tires)*. ČVUT, Praha, 71pp. (in Czech)
- Faria, L.O. & Oden, J.T. 1992. Tire modelling by finite elements. *Tire Science and Technology* **20**(1), 33–56.
- Grečenko, A. 1995. Tyre footprint area on hard ground computed from catalogue values. *Journal of Terramechanics* **32**(6), 325–333.
- Koutný, F. 2009. *Geometry and mechanics of pneumatic tires*. UTB, Zlín, 142 pp. (in Czech)
- Krmela, J. 2008. *Systémový přístup k výpočtovému modelování pneumatik I (System approach to computational modelling of tyres – I. Part)*. Tribun EU, Brno, 102 pp. (in Czech)
- Noor, A.K. & Peters, J.M. 1995. Reduction technique for tire contact problem. *Computer and structures* **60**(2), 223–233.
- Roth, J. & Daar, M.J. 2012. Measurement of normal Stresses at the soil-tire interface. *Agricultural and Biosystems Engineering* **55**(2), 325–331.
- Schreiber, M. & Kutzbach, H. 2008. Influence of soil and tire parameters on traction. *Research in Agricultural Engineering* **54**(2), 43–49.
- Zhang, X., Rakheja, S. & Ganesan, R. 2002. Stress analysis of the multi-layered system of truck tire. *Tire Science and Technology* **30**(4), 240–264.